The Journal of CPRI,
Vol. 5, No. 1, March 2009 pp. 109–119

Performance Analysis of Solar Flat Plate Collectors in Scaling Environment

U C Arunachala*, M Siddhartha Bhatt** and Dr L K Sreepathy***

Scale formation in risers of solar flat plate collectors is evident in places where hard water is being used. This affects both the component functioning as well as system performance. In this paper, the influence of scale deposition on instantaneous efficiency, mass flow rate and heat transfer rates are analysed by the Hottel-Whillier-Bliss (H-W-B) equation in both natural and forced circulation systems. It is observed that variation of mass flow rate affects collector efficiency more than variation of heat transfer rates.

Key words: *solar flat plate water collector, scaling, hardness, instantaneous efficiency, natural circulation systems, forced circulation systems*

1.0 INTRODUCTION

Solar radiation is a term used to describe visible and near-visible (ultraviolet and near-infrared) radiation emitted from the sun. Outside the earth's atmosphere, solar radiation has an intensity of approximately 1370 W/m^2. This is the value at mean earth-sun distance at the top of the atmosphere and is referred to as the Solar Constant [1]. On the surface of the earth on a clear day, at noon, the direct beam radiation will be approximately 1000 W/m^2 for many locations. The solar energy collected in a day in a few cities in India is given in Table 1 [2].

A Solar Flat Plate Water Collector (FPC) is a heat exchanger that transforms incident solar radiation into heat by accumulating it within the enclosure through greenhouse effect. A FPC can be designed for applications requiring energy delivery at moderate temperatures up to 100^{o}C. They receive both beam and diffuse solar radiation, do not require tracking of the sun, and require little maintenance.

Although these collectors have been available for many years, there is continuing interest in their development and optimisation using mathematical analysis, especially for various operating conditions and situations. In a FPC nearly 50-80% of the incident solar radiation can be converted into thermal energy.

2.0 SCALING TENDENCY

Hardness results primarily due to the presence of calcium and magnesium in water. This is undesirable if present in excess, because of formation of deposits in the flow passage with time, termed scaling. The hardness values for designated water quality are shown in Table 2 [3].

2.1 Scaling zone

Impurities present in water used for heating purposes in FPC, form deposits in the flow passage, thus impairing heat transfer and fluid flow.

*Dept. of Mech. Engg., Manipal Institute of Technology, Manipal 576 104, INDIA
Email: arunchandavar@yahoo.co.in
** Central Power Research Institute, Bengaluru 560 080, INDIA
***Dept. of Mech. Engg., JNN College of Engineering, Shimoga 577 204, INDIA

For a typical 2 m^2 collector area, occupied by different flow systems and effect of scaling in each is tabulated in Table 3[4].

TABLE 1	
SOLAR RADIATION DATA	
City	**Solar radiation level ($kWh/m^2/day$)**
Delhi	2.71 - 6.40
Mumbai	3.73 - 6.77
Kolkata	3.18 - 5.48
Bengaluru	4.45 - 6.71
Chennai	4.21 - 6.44
Thiruvananthapuram	4.03 - 5.94

TABLE 2		
HARDNESS OF WATER IN TERMS OF DISSOLVED SOLIDS (ppm)		
S. No.	**Description of water**	**Hardness**
1	Soft water	0-50
2	Moderately soft	50-100
3	Neither hard nor soft	100-150
4	Moderately hard	150-200
5	Hard water	200-300
6	Very hard	above 300

3.0 HOTTEL WHILLIER BLISS (H-W-B) EQUATION

Hottel Whillier Bliss (H-W-B) equation is used to determine the instantaneous efficiency of FPC.

$$\eta_n = F_R\left(\frac{A_p}{A_c}\right)\left[(\tau\alpha) - U_l\,\frac{(T_1 - T_a)}{I}\right] \qquad (1)$$

Since the values of F_R, $(\tau\alpha)$, (A_p/A_c) and U_l are essentially constant, it is seen from equation (1) that if η_n is plotted against $(T_l - T_a)/I$, the intercept would give the value of $[F_{R.}(\tau\alpha)(A_p/A_c)]$, while the slope of the line would give the value of $[F_{R..}\ U_l(A_p/A_c)]$. Equation (1) is rewritten as:

$$\eta_n = a0 - a1\left[\frac{(T_1 - T_a)}{I}\right] \qquad (2)$$

The overall heat loss coefficient for the collector is:

$$U_l = U_t + U_b + U_s \qquad (3)$$

The collector efficiency factor is the ratio of the heat resistance from the absorber plate to the ambient air to the heat resistance from the fluid to the ambient air [5].

$$F' = \frac{1}{W.U_l\left[\frac{1}{U_l[(W-d_o)\phi + d_o]} + \frac{1}{\pi.d_S h} + \frac{1}{2\pi.k_r/\ln(d_o/d_i)} + \frac{1}{2\pi.k_S/\ln(d_i/d_S)}\right]} \qquad (4)$$

Absorber plate effectiveness, φ is given by:

$$\phi = \frac{\tanh\left[M\,(W - d_o)/2\right]}{\left[M\,(W - d_o)/2\right]} \qquad (5)$$

Where,

$$M = \left(\frac{U_l}{k_p.\delta_p}\right)^{1/2} \qquad (6)$$

The collector heat removal factor which measures the thermal resistance encountered by the absorbed solar radiation in reaching the collector fluid is given by:

$$F_R = \frac{\dot{m}.Cp}{U_l.A_p}\left\{1 - \exp\left[-\frac{F'.U_l.A_p}{\dot{m}.Cp}\right]\right\} \qquad (7)$$

Equation (4) calculates the collector efficiency factor in the case of a scaled FPC. But in the case of a clean FPC, the thermal resistance due to scaling tends to, as shown in Figs. 1a and 1b. Typical values of a_0 and a_1 for different types of collectors are given in Table 4 [6].

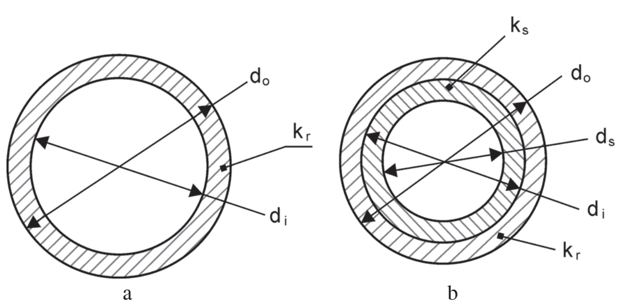

FIG. 1 RISER WITHOUT AND WITH SCALE FORMATION

TABLE 3

SCALING EFFECT IN DIFFERENT ZONES OF THE COLLECTOR

Sl. No.	Scale zone	Total area (m^2)	Scaling effect
1	Risers	0.588	Severe effect on mass flow rate, pressure drop and rise in plate temperature.
2	Headers	0.125	Lesser effect due to larger diameter and less flow area.
3	Storage tank	1.732	Advantageous due to increased thermal resistance between water in the tank and the surrounding air.

TABLE 4

a_0 AND a_1 VALUES FOR VARIOUS COLLECTORS

Type of collector	H-W-B constants	
	a_0	a_1
Owens Illinois evacuated tubular	0.56	4.5
Heywood single cover	0.92	13.25
Heat pipe	0.95	5.0
Philips evacuated tubular	0.72	6.75
Honeywell double selective	0.70	5.62
Flat plate collector	0.75	16.04

4.0 CASE STUDY

A case study on performance evaluation of FPC was undertaken in interior places of Karnataka where the water hardness level is alarming and the working condition of more than 50 FPCs was viewed. It reflected that the performance degradation of FPCs is mainly due to scaling than other parameters like masking of glass cover, absorber plate degradation, leakage from risers, etc. Scale growth of 1 mm to 4 mm in riser, was noticed for the hardness level of 150 ppm–2000 ppm for the working period of 6 months to 8 years.

Attempt to co-relate the experimental data of time period of operation and hardness (ppm) with its scale thickness is under progress.

5.0 EFFECT AND QUANTIFICATION OF SCALE

The typical FPC is of 2 m^2, where natural circulation system is used. If the water outlet pressure and flow rate are basic necessities or if the rise in pressure drop within the system can't be sustained by the thermosiphon effect as in case of very large systems, forced circulation systems are in use. Due to the higher velocity of flow in the riser in forced circulation system, for the given water hardness level, the scale growth rate is not considerable compared to the natural circulation system.

For simulation, both natural and forced circulations FPCs are considered. In the natural system, a collector of 2m x 1m size is taken for the analysis, and the configuration selected in forced circulation system is 10, parallel connected FPC to a pump.

The effects of scaling are reduction in transfer of heat from the riser wall to the circulating fluid due to increased thermal resistance and reduction in the flow area which increases the pressure drop and the result is reduced water flow rate. These effects are quantified in terms of change in the H-W-B constants (a_0 and a_1).

The assumptions made in the analysis are as follows:

- Steady state heat conduction.
- Constant absorber plate effectiveness.
- Scale deposition only in risers.
- Uniform scale deposition.
- Thermal conductivity of scale composition is constant.
- Uniform absorber plate temperature.

5.1 Effect on pressure change in a system

In this section, the pressure gain and drop characteristics of the collector are determined as a function of mass flow rate and then solved to find the mass flow rate. The mass flow rate decreases with increased scaling because of the restriction in the passage which is quantified here.

The pressure drop in the system comprises of frictional drop in risers and is also due to change in sectional geometry in headers, connecting pipes, pipe fittings and the storage tank. But the larger frictional pressure drop occurs in the risers.

5.1.1 Natural circulation FPC

As the flow regime of the riser is laminar with Reynolds Number in the range of 300 and 1200, the laminar friction factor is taken to evaluate the frictional pressure drop as:

$$\Delta p_{drop} = \frac{\omega f L_r V^2}{2 g d_S} \quad (8)$$

Equation (8) is rewritten in terms of the mass flow rate as:

$$\Delta p_{drop} = \frac{128 L_r \dot{m} \mu}{\rho \pi d_S^4} \quad (9)$$

The instantaneous efficiency of the riser is the ratio between output and input power of the riser:

$$\eta_n = \frac{q_u}{IA_p / n} \quad (10)$$

The useful heat gain from the riser is:

$$= \dot{m} \, Cp \Delta T \quad (11)$$

The pressure difference required for a thermosiphon flow (pressure gain) is due to the density difference between the collector outlet and inlet water [7].

$$\Delta p_{gain} = 0.5 g H(\rho_1 - \rho_2) = 0.5 g H B \Delta T \quad (12)$$

By incorporating equations (2), (10) and (11) in equation (12):

$$\Delta p_{gain} = \frac{0.5 g H B I A_p}{n \dot{m} Cp} \left(a0 - a1 \left((T_1 - T_a) / I \right) \right) \quad (13)$$

For any flow system, if both the thermosiphon/pump pressure gain curve and the pressure drop characteristics of the load are known, the resulting flow rate from the two relationships can be solved [8].

Since both the pressure drop and gain equation are the function of the mass flow rate, the mass flow rate is that which balances the thermosiphon buoyancy force/pumping pressure with the frictional resistance in the circuit [9] as shown in Fig. 2.

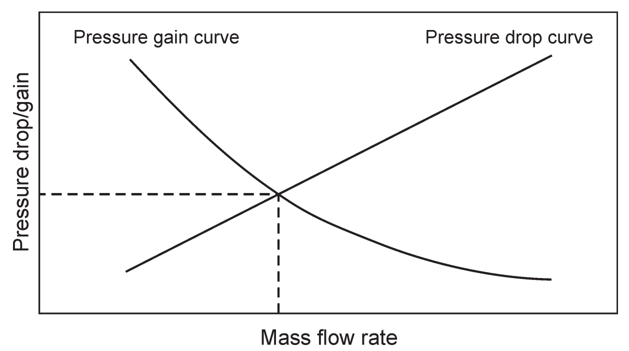

FIG. 2 PRESSURE DROP/GAIN VS MASS FLOW RATE CHARACTERISTICS

The mass flow rate for a clean and scaled riser is derived through an algorithm which is described as follows:

- Since both the pressure drop and pressure gain equations involve $\dot{m}$, by assuming a0 and a1 and considering various collector standard data, mass flow rate is calculated.
- Calculated $\dot{m}$ is taken to determine a new set of a0 and a1 values.
- A new set of a0 and a1 values are reconsidered in $\dot{m}$ calculation.

- Convergent mass flow rate is finalised by iterations.
- In case of scaled condition, the scale modified flow diameter is considered.

5.1.2 Forced circulation FPC

In the case of the forced circulation system, the total pressure drop calculation is based on the weakly turbulent flow as the flow regime of the riser is turbulent with Reynolds Number in the range of 2500 and 6000 and the roughness factor. The pressure drop includes the frictional pressure drop in the riser, suction and delivery pipe of the pump.

$$\Delta p_{drop} = \omega\left[H_r + H_{sd} + \frac{fL_r V^2}{2gd_S}\right] \quad (14)$$

Where, $f = 0.316\mathrm{Re}^{-0.25}$ *; 2300<Re<5000; (15)*

$$f = \frac{1.325}{\left[\ln\left(\frac{\varepsilon}{3.7d_S} + \left\langle\frac{5.74}{\mathrm{Re}^{0.9}}\right\rangle\right)\right]^2} \quad 5000<\mathrm{Re}<10^8 \quad (16)$$

Equation (14) is rewritten in terms of mass flow rate:

$$\Delta p_{drop} = \omega\left[H_r + H_{sd} + \frac{8\, fL_r \dot{m}^2}{\rho^2 g\pi^2 d_S^5}\right] \quad (17)$$

Here, since the pressure gain is due to pump, pump power and overall efficiency are considered to formulate the pressure gain equation in terms of mass flow rate.

$$\Delta p_{gain} = \frac{p_p\,\rho\,.\eta_P}{nm\ \dot{m}} \quad (18)$$

By making use of same algorithm, the one described earlier, true mass flow rate is calculated in the case of a clean and scaled riser.

5.2 Heat transfer analysis

Scaling on a heat transfer surface acts as a layer of insulation, increasing the heat transfer resistance. Significant scaling in solar water heaters will result in increased collector temperatures and thus a degraded system performance. The overall heat transfer resistance depends upon the flow conditions at the heat transfer surface and the magnitude of the wall heat transfer resistance, including any scale [10].

In this section the reduced heat transfer due to scaling is quantified. The mass flow rate calculated from the previous section is considered to determine a_0 and a_1 for different scale conditions.

5.2.1 Natural circulation FPC

Heat loss from the collector to the surrounding is [11]:

$$Q_l = U_l.A_p(T_p - T_a) \quad (19)$$

$$= (S.A_p) - Q_u = (I.\tau.\alpha.Ap) - Q_u \quad (20)$$

Useful heat flow:

$$Q_u = \eta_n I A_p \quad (21)$$

Flowing fluid convective coefficient is derived by the correlation:

$$\mathrm{Nu} = 1.75\left(\frac{\mu}{\mu_w}\right)^{0.14}\left[G_Z + 0.012\left(G_Z.G_r\cos\theta^{0.33}\right)^{1.33}\right]^{0.33} \quad (22)$$

The algorithm to find the convergent value of a_0 and a_1 is described as follows:

- Heat gain and loss by riser is found out by incorporating a_0, a_1, $\dot{m}$, S and A_p.
- Klein's empirical equation is used to find U_t [5].
- For the value of Q_l, U_l and T_p are found out parallely by approximate method.
- By referring appropriate correlation, the convective coefficient of water is calculated.

- Hence F' and F_R are determined.
- New set of values of a_0 and a_1 are calculated.
- These values are reconsidered to get converged values.

5.2.2 Forced circulation FPC

Steps followed to determine a_0 and a_1 are the same except the correlations used to find out the convective coefficient of water:

$$Nu = 0.036 Re^{0.8} Pr^{0.33} \left(\frac{d_S}{L_r} \right)^{0.055} \quad : Re<5000 \quad (23)$$

$$St_B . Pr_B^{0.67} = \frac{f}{8} \quad : Re>5000 \quad (24)$$

6.0 RESULTS AND DISCUSSSION

For the determination of the effect of scaling on various FPC efficiency indicators, the geometric parameters and material properties considered are given in Table 5. Experimental studies are in progress to determine the relationship between scale formation and hardness level of water (ppm) and time period of operation (in years). The results are compared for the scale thickness 1 mm to 4 mm. The algorithm is tested for convergence of a_0 and a_1 values.

If due to thermosiphon effect, the velocity of flow through the tube is considerable i.e. $Gr/Re^2 \approx 1$, then for fluid convective coefficient calculation, combined convection mode is used.

In case of the natural circulation system, the values of a_0 and a_1 are computed for the following cases:

- Effect of heat transfer rate considering the mass flow rate under unscaled condition.
- Effect of mass flow rate considering the heat transfer under unscaled condition.
- Combined effect of mass flow rate and heat transfer rate.

The separate calculation considering only thermal resistance and mass flow rate is to show the effect of each term.

The results of the performance indicators a_0 and a_1 in case of natural circulation system are shown in Table 6. It reflects the dominance of the effect of mass flow rate compared to the effect of heat transfer rates. The variation of efficiency indicators in case of natural circulation FPC given in Table 7 and Table 8 shows the same in the case of forced circulation FPC.

Fig. 3 represents the variation of the overall heat loss coefficient with scale thickness. It can be seen that as the mass flow rate reduces, the absorber plate temperature increases hence the overall heat loss coefficient. Fig. 4 reflects the variation of mass flow rate with scale thickness. It can be observed that in the case of natural circulation system, the percentage reduction in total mass flow rate is 64% for the scale growth of 2 mm and it goes up to 96% for 4 mm growth of scale. But in the forced circulation system, the percentage reduction in total mass flow rate is 53% for scale growth of 4 mm. This is because the mass flow rate is independent of the thermosiphon effect. Fig. 5 shows the variation of pressure drop along the riser with scale thickness. It is seen that the pressure drop along the riser shoots up sharply with scale growth in case of a natural circulation system. Fig. 6 gives the variation of pressure drop with scale growth in the forced circulation system. It is observed that pressure drop along the riser is not considerable up to 3 mm scaling, which indicates that the flow rate changes with scaling is minimum due to pumping power. Thereafter, with severe scaling, pressure drop increases due to lesser flow area. Figs. 7 and 8 show the variation of a_0 and a_1 with scale thickness. It is seen that in the case of the forced circulation system, the drop in the values of a_0 and a_1 with scale growth is not considerable as the heat carrying capacity is not reduced considerably due to less variation in mass flow rate. But in the natural circulation system, the drop in the heat carrying capacity is considerable so that with scale thickness, a_0 and a_1 values reduce.

TABLE 5

GEOMETRIC PARAMETERS AND MATERIAL PROPERTIES

Sl. No.	Term	Symbol	Value	Unit
01	Collector gross area	A_c	2.05	m^2
02	Absorber plate area	A_p	2.0	m^2
03	Collector riser tube length	L	2.0	m
04	Outer diameter of the riser tube	d_o	0.0125	m
05	Inner diameter of the riser tube	d_i	0.0104	m
06	Riser tube pitch	W	0.12	m
07	Riser fin thickness	δ_p	0.7×10^{-3}	m
09	Absorber plate absorptivity	$\acute{\alpha}$	0.95	—
10	Absorber plate emissivity	ε	0.95	—
11	Glass cover transmissivity	τ	0.95	—
12	Absorber plate effectiveness	φ	0.98	—
13	Collector inclination	θ	28.5	°
14	Number of risers	n	9	—
15	Total flux incident on the collector top cover	I	850	W/m^2
16	Collector bottom loss coefficient	U_b	0.58	W/m^2K
17	Collector side loss coefficient	U_s	0.178	W/m^2K
18	Water inlet temperature	T_1	333	K
19	Ambient temperature	T_a	298	K
20	Thermal conductivity of scale material	k_S	2.94	W/mK
21	Thermal conductivity of tube and fin material	k_r	385	W/mK
22	Density of water at inlet temperature	ρ_1	983.2	kg/m^3
23	Viscosity of water at inlet temperature	µì	4.70×10^{-4}	$N.s/m^2$
24	No. of collectors in forced circulation*	m	10	—
25	No. of collectors in thermosiphon circulation	m	1	—
26	Electrical power input to pump*	Pp	185	W
27	Overall efficiency of the pump*	ηo	50	%
28	Pressure head due to suction and delivery pipe	H_{sd}	7.5	m
29	Scaled surface roughness	$\acute{\varepsilon}$	2.5×10^{-5}	m

*Refer to forced circulation collector only

TABLE 6

VALUES OF H-W-B CONSTANTS (NATURAL SYSTEM)

Scale thickness (mm)	Effect of mass flow rate only		Effect of thermal resistance only		Effect of both mass flow rate and thermal resistance	
δ_s	a0	a1	a0	a1	a0	a1
0	0.83	5.02	0.83	5.02	0.83	5.02
1	0.80	4.93	0.82	5.00	0.80	4.91
2	0.76	4.75	0.81	4.95	0.75	4.70
3	0.66	4.28	0.80	4.89	0.64	4.20
4	0.35	2.46	0.77	4.80	0.34	2.39

TABLE 7

VARIATION OF EFFICIENCY INDICATORS WITH SCALING (NATURAL SYSTEM)

Scale thickness	Riser flow diameter	Total mass flow rate	Pressure drop along the tube	Reynolds No.	Plate mean temp.	Overall heat loss coeff.	Collector efficiency factor	Collector heat removal factor	Overall heat transfer Coeff.	H-W-B constants	
δ_S	ds	mt	Δpdrop	Re	T_p	U_l	F'	F_R	U_{OV}	a0	a1
mm	m	kg/h	Pa	—	K	W/m²K	—	—	W/m²K	—	W/m²K
0	0.0104	139	14.30	1176	341	5.46	0.95	0.92	5.19	0.83	5.02
1	0.0084	89	21.50	958	345	5.53	0.93	0.89	5.16	0.80	4.91
2	0.0064	50	35.83	744	350	5.63	0.91	0.83	5.13	0.75	4.7
3	0.0044	22	70.19	537	360	5.82	0.87	0.72	5.09	0.64	4.2
4	0.0024	05	183	305	387	6.38	0.79	0.38	5.00	0.34	2.39

TABLE 8

VARIATION OF EFFICIENCY INDICATORS WITH SCALING (FORCED SYSTEM)

Scale thickness	Riser flow diameter	Total mass flow rate	Pressure drop along the tube	Reynolds No.	Plate mean temp.	Overall heat loss coeff.	Collector efficiency factor	Collector heat removal factor	Overall heat transfer Coeff.	H-W-B constants	
δ_S	ds	mt	Δpdrop	Re	T_p	U_l	F'	F_R	U_{OV}	a0	a1
mm	m	kg/h	Pa	—	K	W/m²K	—	—	W/m²K	—	W/m²K
0	0.0104	3382	9.30	2533	338	5.39	0.97	0.95	5.21	0.86	5.16
1	0.0084	3372	9.41	3127	338	5.40	0.96	0.95	5.19	0.85	5.13
2	0.0064	3334	9.86	4058	339	5.41	0.95	0.94	5.17	0.85	5.10
3	0.0044	3073	13.11	5449	340	5.44	0.94	0.93	5.14	0.84	5.08
4	0.0024	1798	39.44	5941	343	5.49	0.93	0.90	5.09	0.81	4.97

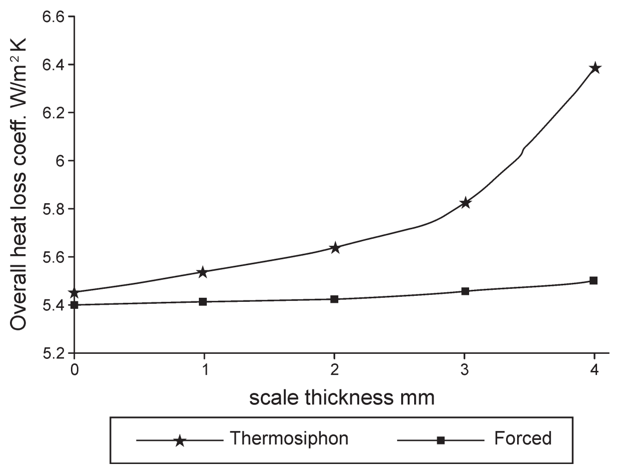

FIG. 3 VARIATION OF OVERALL HEAT LOSS COEFFICIENT WITH SCALE THICKNESS

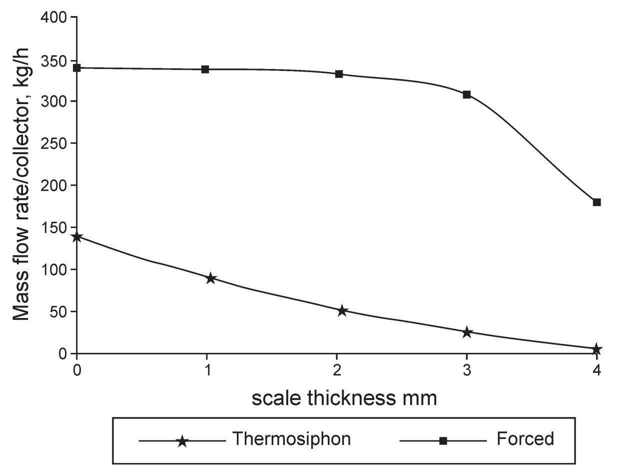

FIG. 4 VARIATION OF MASS FLOW RATE WITH SCALE THICKNESS

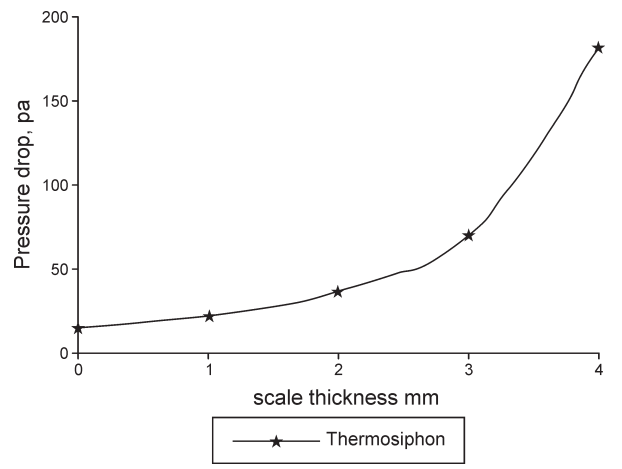

FIG. 5 VARIATION OF PRESSURE DROP ALONG THE RISER WITH SCALE THICKNESS

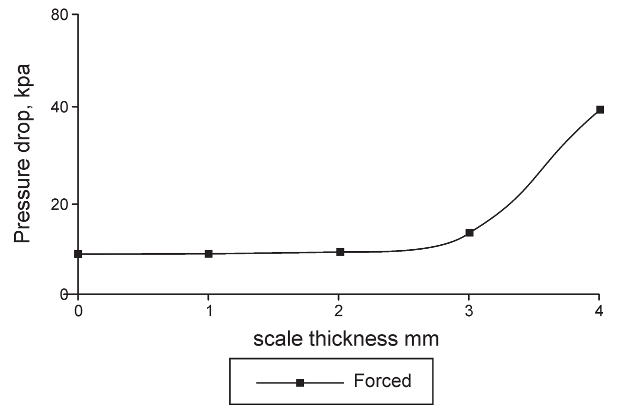

FIG. 6 VARIATION OF PRESSURE DROP ALONG THE RISER WITH SCALE THICKNESS

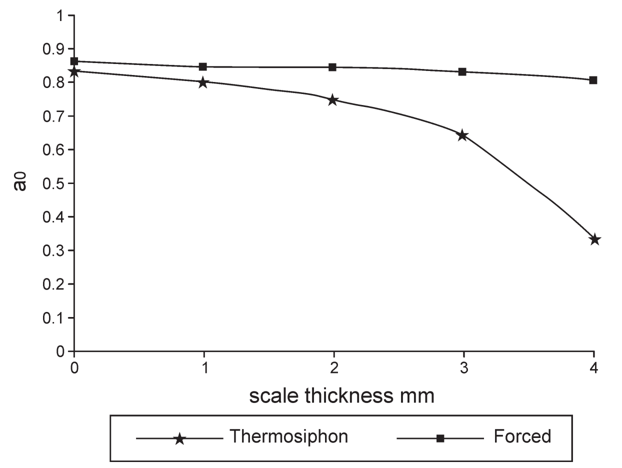

FIG. 7 VARIATION OF a_0 WITH SCALE THICKNESS

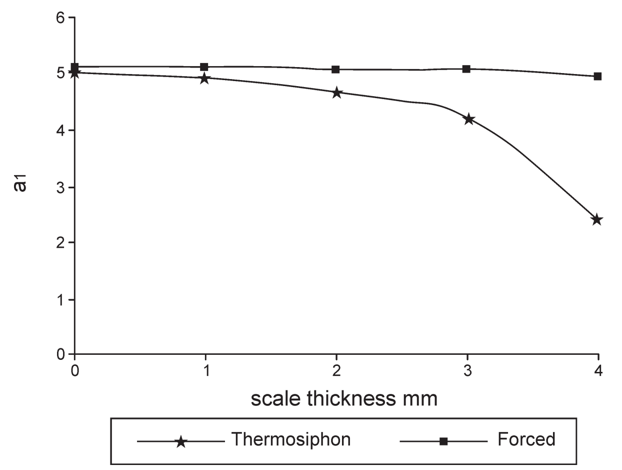

FIG. 8 VARIATION OF a_1 WITH SCALE THICKNESS

7.0 CONCLUSIONS

The conclusions from this study are,

- The collector performance deterioration caused by scaling is due to increased thermal resistance and reduced mass flow rate in the riser.
- The sensitivity of scale induced change in mass flow rate on energy efficiency is more prominent than that of scale induced heat transfer rate.
- In the case of the natural circulation system, the percentage reduction in the total mass flow rate is 64% for scale growth of 2 mm and it goes up to 96% in case of 4 mm growth of scale and the percentage reduction in total mass flow rate is 53% for scale growth of 4 mm in forced circulation collector.
- Even though various descaling techniques are presently available for the solar water heaters, there is a need for technology development.

8.0 NOMENCLATURE

a_0 Intercept of the H-W-B equation (dimensionless)

a_1 Slope of H-W-B equation (W/m^2K)

A Area (m^2)

B	Constant relating density to temperature (kg/m^{3}K)
C_p	Specific heat of water (kJ/kgK)
d	Diameter (m)
f	Friction factor (dimensionless)
F′	Collector efficiency factor (dimensionless)
F_R	Collector heat removal factor (dimensionless)
Gr	Grashof number of water in riser (dimensionless)
G_Z	Graetz number of water in riser (dimensionless)
h	Convective coefficient of water in riser (W/m^{2}K)
H	Height (m)
I	Total flux incident on the top glass cover (W/m^2)
k	Thermal conductivity of material (W/mK)
L	Length (m)
m	Number of collectors (dimensionless)
M	Variable factor in absorber plate effectiveness (m^{-1})
n	Number of risers in a collector (dimensionless)
Nu	Nusselt number of water in riser (dimensionless)
Δp	Pressure change in riser (N/m^2)
P	Collector specific power (kW/m^2)
Pp	Pump power (W)
Pr	Prandtl number of water in riser (dimensionless)
q	Heat gain in riser (W)
Q	Heat flow in collector (W)
Re	Reynolds number of water in riser (dimensionless)
S	Incident solar flux absorbed by the plate (W/m^2)
St	Stanton number of water in riser (dimensionless)
T	Temperature (K)
U	Collector heat transfer coefficient (W/m^{2}K)
V	Fluid velocity in riser (m/s)
W	Pitch of risers (m)
$\dot{m}$	Mass flow rate of water in riser (kg/s)
mt	Total mass flow rate in collector (kg/h)
ΔT	Water temperature diff. in riser(K)

Greek Symbols

α	absorber plate absorptivity (dimensionless)
δ	thickness (m)
ε	surface roughness (m)
η	efficiency (%)
θ	collector orientation (degree)
μ	dynamic viscosity of water (Ns/m^2)
ρ	mass density of water (kg/m^3)
τ	glass cover transmissivity (dimensionless)
	absorber plate effectiveness (dimensionless)
ω	weight density of water (N/m^3)
ϕ	

Subscripts

a	ambient air
b	bottom
B	bulk mean temperature
c	collector
drop	drop
gain	gain
i	inner
l	loss
n	instantaneous
o	outer
ov	overall
p	absorber plate
r	riser
s	side

s scaled

sd pump suction and delivery pipe

t top

u useful

w wall temperature

1 inlet water

2 outlet water

REFERENCES

[1] Aden B Meinel and Marjorie P Meinel, "Applied Solar Energy: An Introduction", Addison–Wesley Publishing Company, Philippines, pp. 41-42, (1977).

[2] N M Nahar, "Year Round Performance and Potential of a Natural Circulation Type of Solar Water Heater in India", Energy and Buildings 35, pp. 240-241, 2003.

[3] K S Venkateswarlu, "Water Chemistry; Industrial and Power Station Water Treatment", New age International Publications, pp. 10-12, (1999).

[4] G L Morrison and J E Braun, "System Modeling and Operation Characteristics of Thermosyphon Solar Water Heaters", Solar Energy, Vol. 34, pp. 389-405, 1985.

[5] J A Duffie and W A Beckman, "Solar Energy Thermal Processes", John Willey, Willey, NewYork, pp. 142-148, (1991).

[6] J C McVeigh, "An Introduction to the Application of Solar Energy, Pergamon Press, London, pp. 51-52, (1977).

[7] G L Morrison and B J Ranatunga, "Thermosyphon Circulation in Solar Collectors", Solar Energy, Vol. 24, pp. 191-198, 1980.

[8] Robert F Boehm, "Design Analysis of Thermal Systems", John Wiley and Sons, New York, pp. 168-170, (1987).

[9] M P Malkin, S A Klein, J A Duffie and A B Copsey, "A Design Method for Thermosyphon Solar Domestic Hot Water Systems", ASME, Vol. 109, pp. 150-155, 1987.

[10] Derek Baker and Gary Vliet, "Designing Solar Hot Water Systems for Scaling Environment", Solar Energy Engg. Published by ASME, Vol. 183, pp. 43-46, 2001.

[11] Larry O Degelman, "Calibrated Simulation of a Solar Hot Water Heater System to Match Degraded Performance Over a 22-year Period using Two Models", Building and Environment (43), pp. 628-637, 2008.

Readers are invited to offer their comments on the article. Please fill in the Reader's Forum.